



Development of a Multiple Wake Model Based on Rapid Recovery Factor in Intense Overlap Case

Bellat Abdelouahad¹, Mansouri Khalifa¹, Raihani Abdelhadi¹

¹Signals, Distributed Systems and Artificial Intelligence Laboratory, ENSET of Mohammedia, Hassan II

University of Casablanca, Morocco.

bellatabdelouahad@gmail.com, khmansouri@hotmail.com, abraihani@yahoo.fr

ABSTRACT

This article studies the influence of wake models on the efficiency of wind farm design, and then the inability of wake models to accurately predict the energy produced by wind farms in the areas of wake interaction. Indeed, all models used in engineering to simulate interaction effect are analytical models based on simple superposition hypotheses. Those models do not take into account the level of turbulence in these areas and to remedy this phenomenon. A factor in mixing square was injected into the classic interaction model of the energy balance, which is also expressed as a function of the speed squares and which makes it possible to recover the speed during a multiple wake. This factor is expressed by an empirical formula as a function of the average diameters and the distances between turbines.

The proposed new model is validated using data from Lillgrund offshore wind farms. So, the achieved results have shown that the proposed approach performs better than the other methods in previous studies.

Key words: Wakemodels, wind farms, interaction effect, turbulence, multiple wake

1. INTRODUCTION

Inside a wind farm, the aerodynamic interaction between the wind turbines induced has a speed deficit called wake and it is divided into a near and far wake. According to Sørensen et al. [1] The downstream turbines located in the wake suffer from this speed deficit and consequently produce less energy compared to the undisturbed conditions. Consequently, the average power losses of wind farms due to the wake of wind turbines are of the order of 10 to 20% in large offshore wind farms. For a low turbine spacing, as in the case of the Lillgrund offshore wind farm, the power loss can reach up to 23%. Besides, several numerical and experimental studies have revealed an increased level of turbulence intensity in the wake [2].

One of the pioneering analytical single wake models is the one proposed by N.O. Jensen [3] in 1983. The model is based on the conservation of momentum and assumes a uniform velocity profile inside the wake. Furthermore, it includes a constant approximated thrust coefficient. Katic et al. [4]

further developed this model in 1986 taking wind turbine characteristics such as a variable thrust coefficient into account. This model is widely known as the Jensen model or PARK model. Later, in 1988 G.C. Larsen [5] proposed a Gaussian-shape wake model, which is based on Prandtl's turbulent boundary layer equation. Larsen himself improved this model in 2009 by applying empirically determining boundary conditions. In 2004, Ishihara et al. [6] developed a wake model, which for the first time takes the effect of turbulence intensity in the wake of the wake recovery into account. Subsequently, in 2006, Frandsen et al. [7] proposed another top-hat shape single wake model for modeling of wind farm efficiencies. A recently developed analytical wake model is the one proposed by Bastankah & Porté-Agel [8] in 2014. The model predicts a Gaussian wake shape and is derived by applying mass and momentum conservation. One of the newest analytical wake models is the one proposed by Gao et al. [9] in 2016. It is based on the Jensen model using a Gaussian wake shape. Furthermore, the model includes a new turbulence intensity model, which takes ambient and rotor added turbulence intensity into account.

It should also be noted that the simplifying hypotheses make the models not precise even the models which simulate the interaction effect of different wakes in the superposition zones. There are four superposition models available: the geometric superposition model (GS), the linear superposition model (LS) proposed by Lissaman [10], the sum of squares model (SS) presented by Katic [11] and the energy balance model (EB) developed by Voutsinas [12], the only distinction lies in the different mathematical expressions of the wake deficits of wind turbines.

Erik [13] and Tian [14] concluded after comparison that the SS model remains the most precise compared to the other models.

In the rest of this study, we will first compare the different wake models in energy prediction and in the development wake, then compare the uncertainties of each model. Secondly a proposal for a new interaction model which considers the effect of the increase in the turbulence intensity in the superimposed area and which corrects the models proposed in previous studies. finally, a validation of our model using the data from the Lillgrund offshore wind farms.

2. WAKE MODELS

2.1 Jensen model

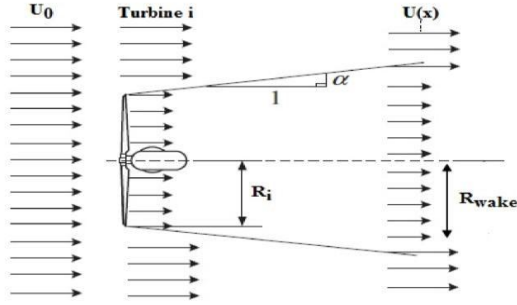


Figure 1: Jensen model principal

The speed deficit in the wake of the wind can be expressed as follows:

$$U_{wake} = U_{In} \left[(1 - \sqrt{1 - C_T}) \left(\frac{R_i}{R_{wake}} \right)^2 \right] \quad (1)$$

$$R_{wake,ij} = R_i + \alpha \Delta x_{ij}$$

Where

- U_{wake} : Wind velocity in the wake area
- U_{In} : incoming wind speed
- C_T : Thrust coefficient
- R_i : Rotor radius
- R_{wake} : Wake radius
- Δx_{ij} : Distance separate wind turbines
- α : Wake decay constant

According to Katic *et al.* [4] α depends on the ambient turbulence.

2.2 Ishihara model

Ishihara conducted a wind tunnel test using a 1/100 scale model of Mitsubishi's MWT-1000 in 2004.[15]-[6] and proposed a new wake model with a Gaussian wind profile by combining the measured wake data and the momentum conservation equation. He constructed a wake model through the wind tunnel test using a scaled wind turbine with a rotor diameter of 57 cm, considering variations of the thrust coefficient and the ambient turbulence intensity. However, since the blade pitch angle of the wind turbine model was fixed, the tip speed ratio of the model had to be adjusted to change the thrust coefficient to cover the wake in the above-rated wind speed region. This operating condition is different from that of general modern megawatt class wind turbines with active pitching.

This model predicts the wake for any ambient turbulence and thrust coefficient.

$$U_{wake} = U_{In} \frac{C_T^{1/2}}{32} \left(\frac{1.666}{k_1} \right)^2 \left(\frac{\Delta x_{ij}}{D_r} \right)^{1-P} \exp \left(\left(\frac{R_r}{R_{wake}} \right)^2 \right) \quad (2)$$

$$R_{wake} = k_1 \frac{C_T^{1/4}}{0.833} D_r^{1-P/2} \Delta x_{ij}^{P/2} \quad (3)$$

$$P = k_2 (I_a + I_w) \quad (4)$$

$$I_w = k_3 \frac{C_T}{\max(I_a, 0.03)} \left(1 - \exp \left(-4 \frac{\Delta x_{ij}}{10 D_r} \right)^2 \right) \quad (5)$$

$$k_1 = 0.27, k_2 = 6.0 \text{ and } k_3 = 0.004 \quad (6)$$

Where

D_r : Rotor diameter

I_a : Ambient turbulence

I_w : Mechanical generated turbulence

2.3 Frandsen model

The Frandsen model is based in a cylindrical control volume with constant cross-sectional is equal to the wake region [7]. The shape of the flow speed can be shown by a constant distribution (top-hat velocity profile). A unique characteristic of this model is the consideration of the initial expansion of the wake. The velocity decay is described as:

$$A_{initial,wake}(x=0) = \beta A_r \quad (7)$$

$$\beta = \frac{1 + \sqrt{1 - C_T}}{2 \sqrt{1 - C_T}} \quad (8)$$

$$A_r = \frac{\pi}{4} D_r^2 \quad (9)$$

$$A_w = \frac{\pi}{4} D_{wake}^2 \quad (10)$$

Where

β : Wake expansion

A_r : Rotor area

A_w : Wake area

The wake deficit at any distance can be written as:

$$U_{wake} = U_{IN} \left[\frac{1}{2} \pm \frac{1}{2} \sqrt{1 - 2 \frac{A_r}{A_w} C_T} \right] \quad (11)$$

Where "+" applies when $C_T \leq 0.75$ and "-" when $C_T \geq 0.75$

$$D_{wake} = \left(\beta^{k/2} + \alpha \frac{\Delta x_{ij}}{D_r} \right)^{1/k} D_r \quad (12)$$

2.4 Gauss model

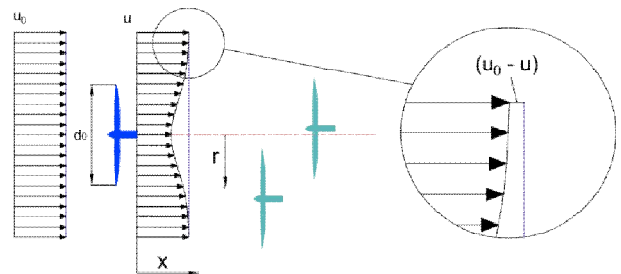


Figure 2: Velocity profile of the wind behind a wind turbine calculated by the GWM.

This wake model based on a Gaussian curve is used to predict the speed deficit caused by wind turbines [16]. This model was proposed by Bastankhah and Porte-Agel [8] and is based on the principle of the law of mass conservation and law of conservation of momentum.

The GWM is based on the following equation for calculating the normalized velocity deficit:

$$\frac{\Delta U}{U_0} = c(x) f\left(\frac{r}{\delta(x)}\right) \quad (13) \quad \frac{\Delta U}{U_0} = c(x) \exp\left(\frac{-r^2}{2\sigma^2}\right) \quad (14)$$

$$C(x) = 1 - \sqrt{1 - \frac{c_t}{8\left(\frac{\sigma}{d_0}\right)^2}} \quad (15)$$

$$\frac{\sigma}{d_0} = k^* \frac{x}{d_0} + \varepsilon \quad (16)$$

$$\frac{\Delta U}{U_0} = \left(1 - \sqrt{1 - \frac{c_t}{8\left(k^*\frac{x}{d_0} + \varepsilon\right)^2}}\right) \times \exp\left(\frac{-1}{2\left(k^*\frac{x}{d_0} + \varepsilon\right)^2} \left[\left(\frac{z-z_h}{d_0}\right)^2 + \left(\frac{y}{d_0}\right)^2\right]\right) \quad (17)$$

Where

$c(x)$: represents the maximum normalized velocity deficit at a given downstream distance x .

r : radial distance measured from the center of the wind turbine.

$\delta(x)$: characteristic wake width at a given distance x .

σ : standard deviation of the Gaussian-shaped velocity deficit at a given distance behind the turbine rotor.

$k^* = \frac{\delta\sigma}{\delta x}$ and ε corresponds to the value of $\frac{\sigma}{d_0}$

3. COMPARISON OF THE WAKE MODELS

Some comparisons which have been made in previous studies [17], and which have shown that for wake development the Jensen model predicts a discrete distribution of the speed deficit, while the GWM predicts a continuous distribution based on a Gaussian form [16]. We can also observe that the speed deficit predicted by the GWM is high compared to that predicted by the Jensen model.

Unlike the Jensen model, the GWM represents the speed deficit with a continuous function in the radial direction. It should also be noted from [18] the Frandsen model predicts the highest wake speed and the Larsen model predicts the largest diameter wake. The Ishihara model predicts the lowest wake speed, Kim and Bottasso, [19]. explains the speed deficit for each model as a function of the distance between the turbines. In the far wake, Jensen and Ishihara show a deviation from the mean square error (RMSE) of 44.8% and 26.5% respectively. The reason for this error could be the low ambient turbulence intensity of 0.23%, which is an unrealistic value. Jensen's model might, because of its simplicity, not consider an extremely low value, and Ishihara, as it was based on correlations of wind turbines, might not be considered an unrealistic value. For Larsen, Frandsen, and Schlichting, the accuracy of the models increases considerably with a difference of 6.7%, 8.6%, and 2.0% respectively.

Concerning the impact of the downstream thrust coefficient on the output power [20]-[21], the wake model of Jensen and Gauss model predicts the power produced approximately when the thrust coefficient is low (high wind speed), but that the Frandsen wake model is very sensitive to the variation of the thrust coefficient, it cannot correctly estimate the power.

Tables 1 and 2 show the deviation of the speed decrease in the far wake of the analyzed models under low ambient turbulence intensity, and high ambient turbulence intensity conditions.

Table 1: The values of the deviation of the velocity decay in the far wake of the analyzed models under low ambient turbulence intensity

Models	Jensen	Larsen	Frandsen	Ishihara
Error %	45.76	6.69	8.66	27.16

Table 2: The values of the deviation of the velocity decay in the far wake of the analyzed models under high ambient turbulence intensity conditions

Models	Jensen	Larsen	Frandsen	Ishihara
Error %	11.79	18.31	6.07	12.89

We can finally say that the estimated global power of the wind farm, varies according to the reliability of the wake model used then to verify the performance of the analytical models previously modeled to predict the wind speed in the wake region we studied three criteria, the first is the parsimony expressed in the relation (18), which characterizes the inverse of the complexity of the model, the second the precision of the estimation of the wake model compared to the experimental data, and the third Imprecision linked to the assumptions and uncertainty on the value of the variables considered in the models. The results are summarized in the two tables 3,4 However, the analysis shows the inability of wake models to predict the speed deficit in the downstream area, due to the uncertainty of the variables considered and its sensitivity to the characteristics of the wind farm.

$$P = \frac{1}{N_{eq} + N_{var}} \quad (18)$$

Where

P: Parsimony

N_{eq} : Number of equations

N_{var} : Number of variables

Table 3: Parsimony estimated of four analytical models

	Parsimony			
	Jensen	Ishihara	Frandsen	Gauss
Number of equations	2	4	7	9
Number of variables	7	13	13	12
Parsimony	1/9	1/17	1/20	1/21

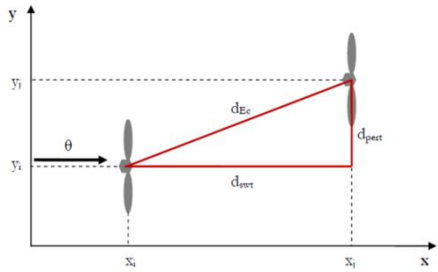
Table 4: Uncertainties of the variables

	Jensen	Ishihara	Frandsen	Gauss
Uncertainly Variables	U_{In}	U_{In}	U_{In}	U_{In}
	C_T	C_T	C_T	C_T
	α	I_a	α	k^*
		I_w	β	β
		k_i	k	ε

We cannot estimate or suppress the wake whatever the model adopted, because these models are based on hypotheses to simplify the calculations. On the other hand, we can standardize the loss of wake of all the wind turbines of a wind farm at similar levels, in order to optimize the power produced and avoid the fatigue of certain blades of wind turbines during the multiple interactions between the wind turbines and which causes a loss of energy in the zones of multiple wake, in the continuation of this study a new model proposed allowing to recover the speed during the interaction between wind turbine.

4. WINDTURBINE INTERACTIONS

In the wind farm, the position of a wind turbine is characterized by Cartesian coordinates (x_i, y_i) as described by equation (19) and illustrated by Figure (3).


Figure 3: Illustration of wind turbine positions in the Cartesian plane

These coordinates are transformed into other coordinates depending on the wind direction that we denote by X_t and Y_t . They are expressed as follows:

$$\begin{cases} X_t(x, y, \theta) = x_i \cos(\theta) + y_i \sin(\theta) \\ Y_t(x, y, \theta) = x_i \sin(\theta) - y_i \cos(\theta) \end{cases} \quad (19)$$

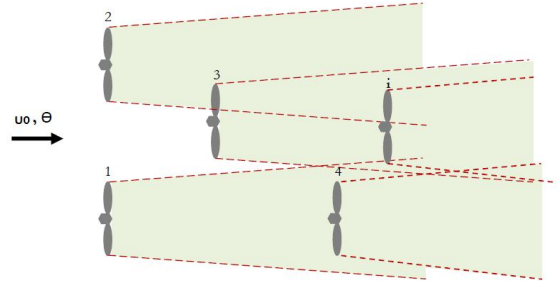
Where

d_{swt} : downstream distance
 d_{pert} : perpendicular distance
 d_{ec} : Euclidean distance

and they are expressed by the equation(20)

$$\begin{cases} d_{swt}(x, y, \theta) = (x_i - x_j) \cos(\theta) + (y_i - y_j) \sin(\theta) \\ d_{pert}(x, y, \theta) = (x_i - x_j) \sin(\theta) + (y_i - y_j) \cos(\theta) \\ d_{ec} = \sqrt{(d_{swt})^2 + (d_{pert})^2} \end{cases} \quad (20)$$

In the wind farm, the downstream wind turbine i can be influenced not only by a single wind turbine but by several wake interferences, generated by the upstream wind turbines Figure (4).


Figure 4: Multiple interactions between wind turbines

Our objective is to develop an interaction model, and which considers the superposition of wake in a wind farm, the models often used to model the interaction of wake are:

$$\text{Geometric Sum (GS)} \quad \frac{U_i}{U_0} = \prod_j^N \frac{U_{ji}}{U_j} \quad (21)$$

$$\text{Linear Sum (LS)} \quad \left(1 - \frac{U_i}{U_0}\right) = \sum_j^N \left(1 - \frac{U_{ji}}{U_j}\right) \quad (22)$$

$$\text{Energy Balance (EB)} \quad U_0^2 - U_i^2 = \sum_j^N (U_j^2 - U_{ji}^2) \quad (23)$$

$$\text{Sum of Squares (SS)} \quad \left(1 - \frac{U_i}{U_0}\right)^2 = \sum_j^N \left(1 - \frac{U_{ji}}{U_j}\right)^2 \quad (24)$$

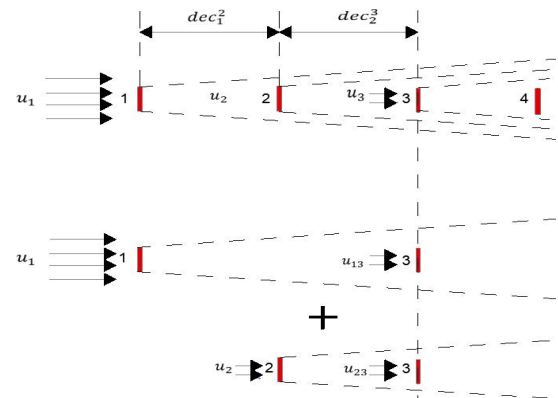
N : the total number of wind turbines that affect the target wind turbine i by their wake

U_i : the inflow speed of the target turbine i

U_j : the wind turbine inflow speed j

U_{ji} : the wind speed at turbine i due to the unique wake of turbine j (obtained by the Jensen empirical model).

Figure 5 shows the superposition of the wake in three scenarios, in fact with the exception of the GS model all the models calculate the loss of wake by superimposing the loss of each wind turbine.


Figure 5: Schematic diagram of three overlapping turbine wakes

Generally, the above models do not consider the increase in turbulence, while previous studies [22]-[23] indicate that the stronger the turbulent ambient intensity, the faster the recovery of wake. Wind tunnel experiments [24]-[25] have also shown that the turbulence intensity in the wake in the wake overlay area is higher than that of the undisturbed wind turbine in the same place. So, to consider this, this study aims at first to multiply the total superimposed loss by a mixing coefficient of less than 1, this allows recovery of the speed caused by the growth of Intensity in the superimposed wake zone. The mixing coefficient can be described by an empirical formula as follows:

$$\beta = 1 - \frac{dt_{aver}}{dec_{aver}} \quad (25)$$

dec_{aver} is expressed by(26),

$$dec_{aver} = \frac{1}{N-1} \sum_{j=1}^{N-1} dec_j^{j+1} \quad (26)$$

$$And dec_j^{j+1} = \sqrt{d_{swt_j}^{j+1} + d_{per_j}^{j+1}} \quad (27)$$

Where

dt_{aver} : is the average diameter when using different types of wind turbines

dec_j^{j+1} : spacing between every two upwind adjacent turbines

dec_{aver} : the average value of dec_j^{j+1}

$d_{swt_j}^{j+1}$: downstream distance

This coefficient allows faster speed recovery by its value which is less than 1 and by its formula which considers the spacing between wind turbines, according to previous studies [26]-[27] a smaller spacing of wind turbines leads to the high intensity of turbulence in the superposed area, hence the inclusion of a mixing coefficient in the EB model and the proposed DEB model can be written by equation (28).

$$U_0^2 - U_i^2 = \beta^2 \sum_j^N (U_j^2 - U_{ji}^2) \quad (28)$$

the square of the value of β is explained by the fact that we reason on the squares of the speeds in the formula EB, other studies [28] have tried to modify the same formula but without introducing the square of the mixing factor ,without taking into account neither the average of the diameters of the turbines for the parks equipped by several types of wind turbine nor the distances separating the wind turbines with the variation of the wind direction, it should also be noted that this mixing coefficient is only applied in the case of a large perturbations in the wake superposition.

5. COMPARATIVE STUDY AND VALIDATION

5.1 Lillgrund Wind Farm

The Lillgrund wind farm is equipped with 48 SWT-2.3-93 Siemens wind turbines with wind rotor diameter of 92.6 m and hub height of 65 m, the distinctive feature of this park is

the very tight configuration of the wind turbines, with a distance separation of 3.3D and 4.3D rotor diameter under the direction of the wind of 120 ° and 222 °, respectively. Below figure 6 which gives the layout of the Lillgrund offshore wind farm.

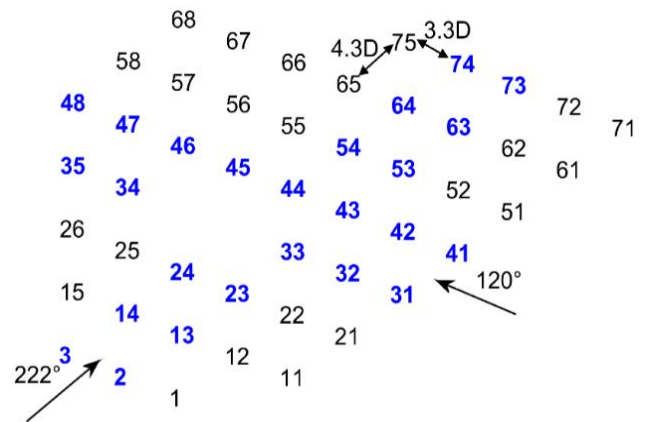


Figure 6: Layout of the Lillgrund offshore wind farm

5.2 Results and Discussion

To test and validate our model, the Jensen model is used in all the interactions studied previously (LS, SS, EB, MEB, DEB), in order to calculate the power deficit while respecting the constraints of the layout of the offshore wind farm of Lillgrund figure 6.

The power deficit of the wind turbine can be defined as $1 - \frac{P_i}{P_0}$, where P_i is the actual power of a specific turbine i and P_0 is the power of a turbine not disturbed, the inflow mean velocity at hub height is 9 m/s in all cases. The wake expansion rate of the Jensen model is set to be 0.05 according to the recommended value for offshore conditions.

The calculations made in this study consider the different wind directions, consistent with those of the inflow sector of processed SCADA (Supervisory control system and data acquisition) data $[-2.5^\circ, 2.5^\circ]$ [29], and are performed in 0.5° steps for both arrays,

the results of this study are given in the four figures 7,8,9 and 10.

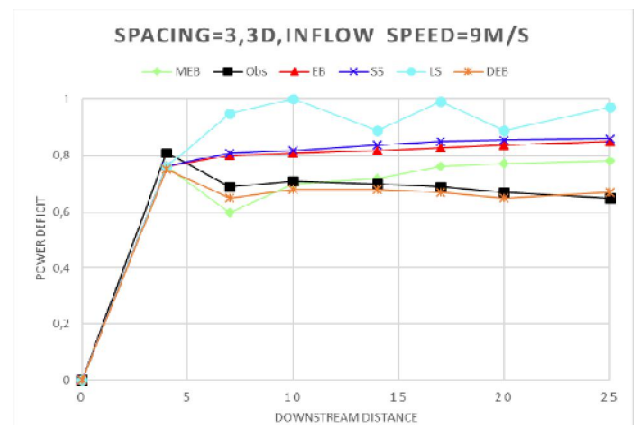


Figure 7: Lillgrund power deficit in a complete row with 3.3D spacing

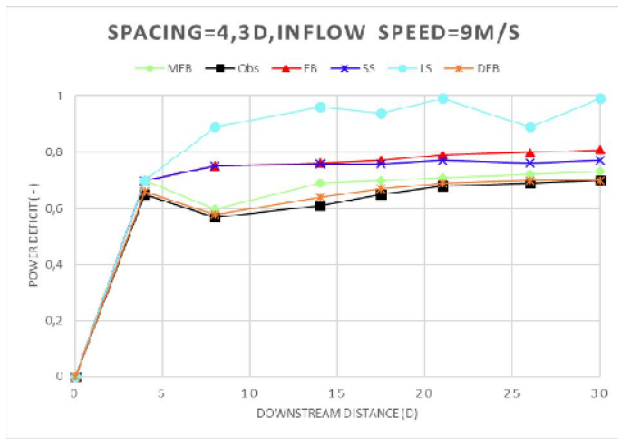


Figure 8: Lillgrund power deficit in a complete row with 4.3D spacing

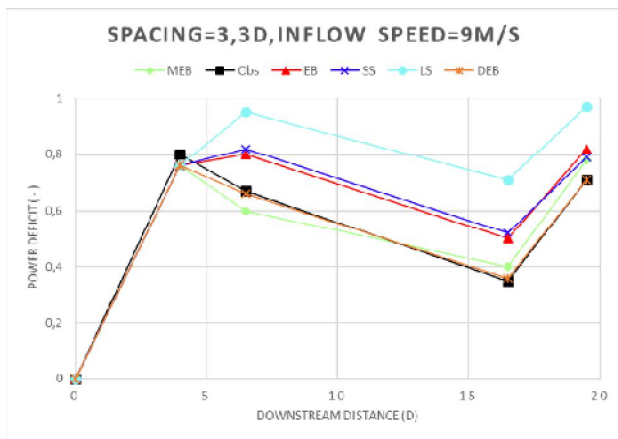


Figure 9: Lillgrund power deficit in a complete row with 3.3D spacing with two missing turbines

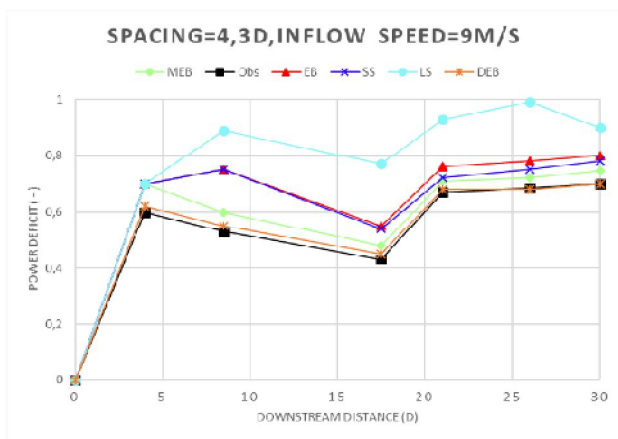


Figure 10: Lillgrund power deficit in a complete row with 4.3D spacing with one missing turbine

The figures above (Figure 7,8,9 and 10), represent the variation of speed deficit of the models for different separation distances of the turbines, we can note in the two figures(7,8) that the deficit is very important and overestimated by the LS model, that is explained by the absence of wake in the case where the input speed is lower than the nominal speed which causes the turbines to stop. The two models SS and EB are almost similar, in the second

turbine all models approach and reach values between 82% and 65% because of the small spacing ,but once we get to the third turbine only our proposed DEB model which perfectly predicted energy recovery, in the case of the spacing of 4.3D the DEB and MEB models are in perfect agreement with the observations, we also note that the proposed DEB model remains a little more precise than the MEB model proposed in [28]. In the case of 3.3D spacing, none of the superposition models could predict the trend of energy recovery after the third turbine except the proposed DEB model, and this confirms the uncertainties and errors induced by the Jensen wake model studied before.

In figures 9 and 10, the curves are different from figures 7 and 8, they tend to regress because of certain turbines which are missing in the studied rows, at the beginning the results remain the same as the previous ones, but from the third turbine at the fourth, the wakes are recovering and our DEB model remains the most precise and in agreement with the measurements, better than the other models in both cases.

To measure the accuracy of the DEB model, note in relation to the wake interaction, the performance indicator used to calculate the efficiency of the wind farm, which is defined as the ratio between the wind farm actual total output power and the power of the wind farm without considering the wake effect, the efficiency can be expressed as:

$$eff = \frac{\sum_i P_i}{NP_0} \quad (29)$$

Where N is the number of wind turbines.

It should be noted here that the Jensen model is integrated with five superposition models, to calculate the efficiency of the fleet in all wind directions with an average speed of 9 m / s in each direction.

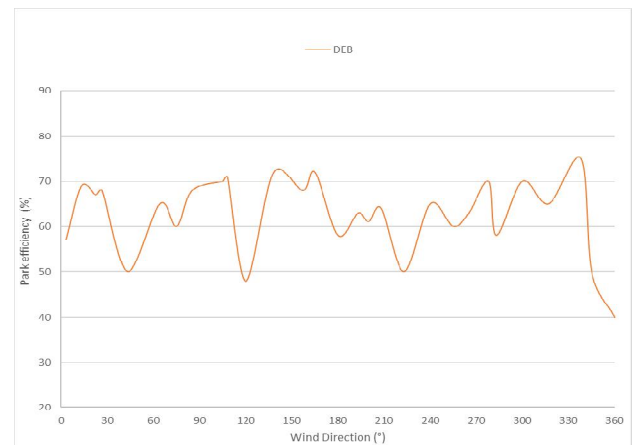


Figure 11: Park efficiency of the Lillgrund farm for the inflow sector 0-360° with 3° increments

According to figure 11, the proposed DEB model correctly predicts the variation in efficiency with the evolution of the wind direction and the location of the extreme points. By comparing this variation with previous studies [28] and calculating the mean square error (RMSE) and the mean absolute percentage error (MAPE) by the formulas below:

$$RMSE = \sqrt{\frac{1}{k} \sum_i^k (eff_{model,i} - eff_{obs,i})^2} \quad (30)$$

$$MAPE = \frac{1}{k} \sum_i^k \left[\frac{eff_{model,i} - eff_{obs,i}}{eff_{obs,i}} \right] \times 100\% \quad (31)$$

Tables 5 and 6 summarize the RMSE and MAPE calculation results. We can say from this table that the efficiency of a wind farm calculated by the DEB model is more precise than the MEB model, in the input sector (0-360 °), the DEB model reduces the RMSE by 4.13% and decreases the MAPE by 6.77% compared to the most commonly used SS model. Besides, these values are reduced by 2.37% and 3.17%, respectively, in the prevailing wind direction range. A remarkable reduction also compared to the MEB model of 0.34% for RMSE and 1.47% for MAPE and in the dominant wind direction range a continuation in the reduction of 0.41% and 0.69% respectively.

Table 5: Simulation error of the park efficiency using different models

Error Models	Prevailing Wind Directions				
	LS	EB	SS	MEB	DEB
Root mean square error (RMSE) (%)	12.55	7.26	8.99	5.2	4.86
Mean absolute percentage error (MAPE) (%)	17.06	9.24	11.78	6.48	5.01

Table 6: Simulation error of the park efficiency using different models

Error Models	Prevailing Wind Directions				
	LS	EB	SS	MEB	DEB
Root mean square error (RMSE) (%)	8.99	4.6	5.07	3.11	2.7
Mean absolute percentage error (MAPE) (%)	12.84	6.2	6.22	3.74	3.05

6. CONCLUSION

In the first part of this study, attempts have been made to compare wake models with a series of numerical simulations of wind turbine wake, and different ambient turbulence intensities and thrust coefficients, indeed none of the analytical wake models can estimate the wind speed deficit approximately, but the Jensen wake model according to this study still the model that gives.

In the second part of this study we tried to choose the Jensen model which validated the criteria of previous study in order to study the power deficit in the case of superposition of the wake, in fact all the conventional models of wake calculate separately the speed deficit of each wind turbine to the wind and then superpose them without considering the faster wake recovery caused by a higher turbulence intensity in the superposed wake region.

All conventional interaction wake models do not consider the faster recovery of the wake caused by a higher intensity of turbulence in the overlapping wake region, and calculate the

speed deficit of each wind turbine separately and then overlap linearly. Our contribution and to improve an energy balance model in order to predict the speed and power distribution of a wind farm for this a mixing coefficient is introduced to characterize the above phenomenon in the energy balance model, and an empirical expression is also given to calculate this parameter.

The Lillgrund offshore wind farm was chosen to validate the proposed model by calculating the power loss of each wind turbine and the efficiency of the wind farms. Our model was compared with other commonly used superposition models in engineering and with the MEB model from a previous study, and showed higher accuracy compared to other models with the same simplicity and cost of computation and better in agreement with the measurements in the park studied, we also note that the square of the coefficient used in this article and injected into the empirical formula has participate in the recovery of wake faster in the overlapping wake area.

REFERENCES

- [1] K. Nilsson, S.-P. Breton, J. N. Sørensen, and al -, "Determination of Wind Turbine Near-Wake Length Based on Stability Analysis Related Content Airfoil data sensitivity analysis for actuator disc simulations used in wind turbine applications," J. Phys. Conf. Ser. OPEN ACCESS.
- [2] T. Ishihara and G. W. Qian, "A new Gaussian-based analytical wake model for wind turbines considering ambient turbulence intensities and thrust coefficient effects," J. Wind Eng. Ind. Aerodyn., vol. 177, pp. 275–292, Jun. 2018.
- [3] N. O. Jensen, "General rights A note on wind generator interaction," 1983.
- [4] I.; Katic, J.; Højstrup, and N. O. Jensen, "A Simple Model for Cluster Efficiency," APA, 1987.
- [5] M. Gaumond et al., "Benchmarking of Wind Turbine Wake Models in Large Offshore Windfarms," in Proceedings of Torque 2012, The science of making torque from wind, 2012.
- [6] T. Ishihara, A. Yamaguchi, and Y. Fujino, "Development of a new wake model based on a wind tunnel experiment," Glob. Wind Power, p. 6, 2004.
- [7] S. Frandsen et al., "Analytical modelling of wind speed deficit in large offshore wind farms," in Wind Energy, 2006, vol. 9, no. 1–2, pp. 39–53.
- [8] M. Bastankhah and F. Porté-Agel, "A new analytical model for wind-turbine wakes," Renew. Energy, vol. 70, pp. 116–123, Oct. 2014.
- [9] X. Gao, H. Yang, and L. Lu, "Optimization of wind turbine layout position in a wind farm using a newly-developed two-dimensional wake model," Appl. Energy, vol. 174, pp. 192–200, Jul. 2016.
- [10] P. B. S. Lissaman, "Energy Effectiveness of Arbitrary Arrays of Wind Turbines.," Journal of energy, vol. 3, no. 6, pp. 323–328, 1979. <https://doi.org/10.2514/3.62441>
- [11] N. Otto, E. Proceedings, and R. A. Raguzzi, "A Simple Model for Cluster Efficiency Publication date : Publisher

- 's PDF , also known as Version of record Link to publication," vol. 1, 1987.
- [12] R.Rados, K.G. Voutsinas, and S.G. Zervos, "Wake effects in wind parks a new modeling approach, " In Scientific Proceedings, EWEC. Travemunde, Germany, 1993; pp. 444–447.
- [13] E. Djerf and H. Mattsson, "Evaluation of the Software Program WindFarm and Comparisons with Measured Data from Alsvik," p. 86, 2000.
- [14] L. Tian, W. Zhu, W. Shen, Y. Song, and N. Zhao, "Prediction of multi-wake problems using an improved Jensen wake model," *Renewable Energy*, vol. 102, pp. 457–469, 2017.
- [15] A. Mittal, L. K. Taylor, K. Sreenivas, and A. Arabshahi, "Investigation of two analytical wake models using data from wind farms," in ASME 2011 International Mechanical Engineering Congress and Exposition, IMECE 2011, 2011, vol. 6, no. PARTS A AND B, pp. 1215–1222.
- [16] L. Parada, C. Herrera, P. Flores, and V. Parada, "Wind farm layout optimization using a Gaussian-based wake model," *Renew. Energy*, vol. 107, pp. 531–541, Jul. 2017.
<https://doi.org/10.2514/6.2012-5430>
- [17] B. Abdelouahad, E. C. M. El Houssine, L. Zahiri, R. Abdelhadi, and K. Mansouri, "Wind farms power estimation based on the different wake models and their optimization," 2020 1st International Conference on Innovative Research in Applied Science, Engineering and Technology, IRASET 2020, 2020.
- [18] W. Tong, S. Chowdhury, J. Zhang, and A. Messac, "Impact of Different Wake Models on the Estimation of Wind Farm Power Generation," 2012.
- [19] H. Kim, K. Kim, C. Bottasso, F. Campagnolo, and I. Paek, "Wind Turbine Wake Characterization for Improvement of the Ainslie Eddy Viscosity Wake Model," *Energies*, vol. 11, no. 10, p. 2823, Oct. 2018.
- [20] L. G. Salgado, "Experimental analysis of analytical wake models for wind turbines."
- [21] N. Charhouni, M. Sallaou, and K. Mansouri, "Design analysis of critical concepts influence wind farm production and efficiency," *Int. J. Eng. Res. Africa*, vol. 40, pp. 136–150, 2018.
- [22] A. Crespo and J. Hernández, "Turbulence characteristics in wind-turbine wakes," *Journal of Wind Engineering and Industrial Aerodynamics*, vol. 61, no. 1, pp. 71–85, 1996.
- [23] A. Duckworth and R. J. Barthelmie, "Investigation and validation of wind turbine wake models," *Wind Engineering*, vol. 32, no. 5, pp. 459–475, 2008.
- [24] A. A. Veisi and M. H. ShafieiMayam, "Effects of blade rotation direction in the wake region of two in-line turbines using Large Eddy Simulation," *Applied Energy*, vol. 197, pp. 375–392, 2017.
- [25] S. Lee, P. Vorobieff, and S. Poroseva, "Interaction of wind turbine wakes under various atmospheric conditions," *Energies*, vol. 11, no. 6, 2018.
- [26] H. Liu, I. Hayat, Y. Jin, and L. P. Chamorro, "On the evolution of the integral time scale within wind farms," *Energies*, vol. 11, no. 1, pp. 1–11, 2018.
- [27] L. P. Chamorro and F. Porté-Agel, "Turbulent flow inside and above a wind farm: A wind-tunnel study," *Energies*, vol. 4, no. 11, pp. 1916–1936, 2011.
- [28] Z. Shao, Y. Wu, L. Li, S. Han, and Y. Liu, "Multiple wind turbine wakes modeling considering the faster wake recovery in overlapped wakes," *Energies*, vol. 12, no. 4, 2019.
- [29] T. Göçmen, P. Van Der Laan, P. E. Réthoré, A. P. Diaz, G. C. Larsen, and S. Ott, "Wind turbine wake models developed at the technical university of Denmark: A review," *Renewable and Sustainable Energy Reviews*, vol. 60, pp. 752–769, 2016.